Author Manuscript

Author Manuscript

Author Manuscript

Author Manuscript

HHS Public Access

Author manuscript

Acta Biomater. Author manuscript; available in PMC 2018 September 15.

Published in final edited form as:

Acta Biomater. 2017 September 15; 60: 210–219. doi:10.1016/j.actbio.2017.07.016.

Micrometer Scale Guidance of Mesenchymal Stem Cells to Form Structurally Oriented Large-Scale Tissue Engineered Cartilage

Chih-Ling Chou[1,*], **Alexander L. Rivera**[2,*], **Valencia Williams**[1], **Jean F. Welter**[3], **Joseph M. Mansour**[4], **Judith A. Drazba**[5], **Takao Sakai**[6], and **Harihara Baskaran**[1]

[1]Department of Chemical Engineering, Case Western Reserve University, Cleveland, Ohio

[2]Department of Biomedical Engineering, Case Western Reserve University, Cleveland, Ohio

[3]Skeletal Research Center, Department of Biology, Case Western Reserve University, Cleveland, Ohio

[4]Department of Mechanical and Aerospace Engineering, Case Western Reserve University, Cleveland, Ohio

[5]Lerner Research Institute, Cleveland Clinic, Cleveland, Ohio

[6]Department of Molecular and Clinical Pharmacology, Institute of Translational Medicine, University of Liverpool, Liverpool, UK

Abstract

Current clinical methods to treat articular cartilage lesions provide temporary relief of the symptoms but fail to permanently restore the damaged tissue. Tissue engineering, using mesenchymal stem cells (MSCs) combined with scaffolds and bioactive factors, is viewed as a promising method for repairing cartilage injuries. However, current tissue engineered constructs display inferior mechanical properties compared to native articular cartilage, which could be attributed to the lack of structural organization of the extracellular matrix (ECM) of these engineered constructs in comparison to the highly oriented structure of articular cartilage ECM. We previously showed that we can guide MSCs undergoing chondrogenesis to align using microscale guidance channels on the surface of a two-dimensional (2-D) collagen scaffold, which resulted in the deposition of aligned ECM within the channels and enhanced mechanical properties of the constructs. In this study, we developed a technique to roll 2-D collagen scaffolds containing MSCs within guidance channels in order to produce a large-scale, three-dimensional (3-D) tissue engineered cartilage constructs with enhanced mechanical properties compared to current constructs. After rolling the MSC-scaffold constructs into a 3-D cylindrical structure, the constructs were cultured for 21 days under chondrogenic culture conditions. The microstructure architecture and mechanical properties of the constructs were evaluated using imaging and

Corresponding Author: Harihara Baskaran, 141C, A.W. Smith Building, 2102 Adelbert Road, Cleveland, OH 44106-7217, Phone: 216 368 1029.

*These authors contributed equally.

Publisher's Disclaimer: This is a PDF file of an unedited manuscript that has been accepted for publication. As a service to our customers we are providing this early version of the manuscript. The manuscript will undergo copyediting, typesetting, and review of the resulting proof before it is published in its final citable form. Please note that during the production process errors may be discovered which could affect the content, and all legal disclaimers that apply to the journal pertain.

Author Manuscript Author Manuscript Author Manuscript Author Manuscript

compressive testing. Histology and immunohistochemistry of the constructs showed extensive glycosaminoglycan (GAG) and collagen type II deposition. Second harmonic generation imaging and Picrosirius red staining indicated alignment of neo-collagen fibers within the guidance channels of the constructs. Mechanical testing indicated that constructs containing the guidance channels displayed enhanced compressive properties compared to control constructs without these channels. In conclusion, using a novel roll-up method, we have developed large scale MSC based tissue-engineered cartilage that show microscale structural organization and enhanced compressive properties compared to current tissue engineered constructs.

Graphical abstract

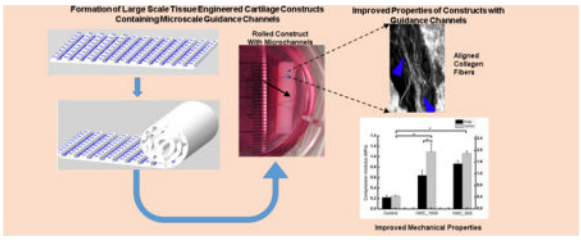

Keywords

Contact Guidance; Chondrogenesis; Large-Scale Constructs; Tissue Engineering; Osteoarthritis

Introduction

Osteoarthritis is a condition that is characterized by the damage of the articular cartilage of the joints, which can result in severe joint discomfort and pain. Due to its avascular nature, self-repair capacity of cartilage is poor and damage to it ultimately results in a mechanically inferior fibrocartilage repair tissue. Tissue engineering has been proposed as a method for the development of cartilage constructs to treat these articular cartilage injuries. Most tissue engineering approaches involve a traditional strategy of culturing scaffolds seeded with mesenchymal stem cells (MSCs) or chondrocytes and growth factors to produce cartilage constructs *in vitro* [1–12]. Many studies have shown that when exposed to chondrogenic factors, MSCs produce an extracellular matrix (ECM) that displays certain biochemical similarities to native cartilage such as richness in collagen type II and glycosaminoglycans (GAG), two of the primary ECM components of native articular cartilage. However, these tissue engineered cartilage constructs are biomechanically inferior to native cartilage and are not suitable for physiological load bearing function. This limitation has been attributed to a lack of an ultrastructure in tissue engineered constructs, which is present in the native tissue. Mathematical models have shown that oriented structures of collagen in cartilage play an important role in determining the mechanical properties of the native tissue [13, 14]. We showed earlier that microscale guidance channels on the scaffold surface can be used to align human mesenchymal stem cells (hMSCs), which then deposited aligned ECM with enhanced mechanical properties [15]. These two-dimensional (2-D) constructs containing guidance channels with oriented hMSCs and aligned ECM showed superior biomechanical properties compared to constructs without guidance channels. The orientation of cells and

Author Manuscript Author Manuscript Author Manuscript Author Manuscript

ECM in the direction of applied force led to a significantly higher modulus of elasticity under tension. However, these 2-D constructs did not provide a solution for three-dimensional (3-D) cartilage defects, and therefore, are not suitable for clinical applications. Indeed, many studies demonstrating efficacy for tissue engineering at the 2-D level are not readily translatable to yield clinically useful 3-D tissue constructs.

The objective of this study was to develop large-scale, clinically-applicable cartilage-like tissue with enhanced mechanical properties compared to current tissue-engineered cartilage. We investigated a novel roll-up method that utilized the cell-ECM adhesive characteristics of MSCs undergoing chondrogenic differentiation to produce structurally oriented 3-D tissue engineered constructs that have microscale guidance channels at the 2-D level. Results show that the roll-up method is an efficient way to translate fine 2-D details down to 50 micrometers in a 3-D construct. Histology and immunohistochemistry results show extensive GAG and collagen type II production, indicative of cartilage-like ECM. Further, mechanical properties of the 3-D constructs were enhanced by the presence of guidance channels. Second harmonic generation imaging and Picrosirius red staining indicate alignment of neo-collagen fibers as a result of microscale guidance.

Materials & Methods

Collagen type I from bovine Achilles tendon, chondroitin-6-sulfate sodium salt from shark cartilage, 1-ethyl-3-(3-dimethylaminopropyl) carbodiimide hydrochloride (EDC), N-hydroxy-succinimide, fetal bovine serum (FBS), 4′, 6-diamidino-2-phenylindole (DAPI), and phalloidin were purchased from Sigma Chemical Co. (St. Louis, MO). Antibiotic-antimycotic cocktail, low glucose Dulbecco's Modified Eagle Medium (DMEM-LG), high glucose DMEM (DMEM-HG), dexamethasone, sodium pyruvate, and human plasma fibronectin were obtained from Gibco, Invitrogen (Carlsbad, CA). Ascorbate 2-phosphate was purchased from Wako Chemicals USA (Richmond, VA), Fibroblast growth factor-2 (FGF) and transforming growth factor β1 (TGF-β1) were purchased from Peprotech (Rocky Hill, NJ). ITS (insulin, transferrin, selenium)+ Premix Tissue Culture Supplement were obtained from Becton Dickinson (Franklin Lakes, NJ), calcein AM, and ethidium homodimer-1 (EthD-1) were obtained from Molecular Probes (Invitrogen, Carlsbad, CA). Fluorescein isothiocyanate (FITC)-conjugated goat anti-mouse IgG secondary antibody was from MP Biomedicals (Irvine, CA,) and Texas Red conjugated goat anti-mouse IgG secondary antibody was from Molecular Probes (Invitrogen, Carlsbad, CA) while the collagen Type I and Type II primary antibodies were obtained from the Developmental Studies Hybridoma Bank (University of Iowa). Sterile 27′ poly-glycolic acid (PGA) absorbable sutures was obtained from Integra Miltex (York, PA)

Collagen-GAG and EDC Solutions

Collagen-GAG solution was made using a previously published homogenization method [15]. Briefly, 2.2 g of type I bovine collagen was dissolved in 800 ml of 0.5% acetic acid in diH_2O by blending in an ice-bath-cooled vessel in a tissue homogenizer (IKA-Works, Wilmington, NC) at a speed of 13,500 rpm for 20 minutes. 0.22 g of chondroitin-6-sulfate in 40 ml of 0.5% acetic acid in diH_2O was then added drop-wise to the homogenized collagen

Author Manuscript Author Manuscript Author Manuscript Author Manuscript

solution. The solution was further homogenized at 22,000 rpm for 20 minutes. A crosslinking solution of EDC was made by dissolving 0.727 g of EDC and 0.063 g of N-hydroxy-succinimide in 100 ml of diH_2O and was used in the pattern formation as described in '*Pattern Formation in Collagen Membrane*'.

Design of Microchannels

Templates for rectangular channels of a constant length, width and varying spacing were created using AutoCAD LT (AutoDesk, San Rafael, CA). One-hundred micrometer wide channels with either 50 or 100 micrometer spacing and 1.5 cm length were used for 3-D roll-up constructs. The 100 micrometer width and the two different spacings were chosen as these were the smallest dimensions we can pattern in collagen with high reliability and accuracy [15]. The depth of the channels was maintained constant, at 70 micrometers. To form these channels on a silicon template, we used standard microfabrication methods as described previously [15].

Pattern Formations in Collagen Membrane

Collagen-GAG membranes of about 100 micrometers thickness were produced using a filtration method over a period of 1 hour. Silicon wafers containing the patterns were then used to produce channels on the surface of the collagen membranes by a previously-published technique of collagen soft-lithography [16]. Briefly, by a technique that involved selective solubilization, patterning, and pattern stabilization through EDC crosslinking, stable microchannel patterns were formed in the collagen-GAG membranes. The membranes were then incubated in 10× antibiotic-antimycotic cocktail for one day and 1× antibiotic-antimycotic cocktail for another day, and then washed thoroughly and stored in PBS until seeding.

Cell Culture

The hMSCs were prepared as previously described from bone marrow aspirates obtained from three healthy adult volunteer donors through the Institutional Review Board (IRB)-approved Stem Cell Core Facility of the Case Comprehensive Cancer Center [17]. The aspirates were harvested after informed consent under the terms of an IRB-approved protocol. The hMSCs were cultured to confluence in DMEM-LG containing 10% FBS and 10 ng/ml FGF-2. The hMSCs were then trypsinized and resuspended at approximately 50×10^6 cells/ml.

Roll-up Collagen-hMSC Construct Formation and Differentiation

The hMSC suspension (50×10^6 cells/ml) was applied to the patterned surface of the collagen membrane (1.8 cm width by 7.2 cm length) using a micropipette. A total of 8.4 million cells were seeded per construct. After a 2 hour period to allow for cell attachment, the seeded membranes were rolled up using forceps to create a multi-layer spiral cylinder construct. The 2-hour seeding procedure allowed for >98% efficiency with respect to cell adhesion to the membrane. Two sterile polyglycolic acid (PGA) absorbable sutures were tied around the construct to ensure contact between the cells and scaffold, and prevent unrolling of the layers, as illustrated in Fig. 1. The dimensions for the final roll-up construct were

Author Manuscript Author Manuscript Author Manuscript Author Manuscript

approximately 1.8 cm (length) by 0.35 cm (diameter). All samples were cultured in chondrogenic differentiation medium for 21 days in a standard incubator at 37 °C and 5% CO_2 in humidified air. The medium was changed every 2–3 days. The chondrogenic differentiation medium consisted of DMEM-HG supplemented with 1% ITS+ Premix Tissue Culture Supplement, 10^{-7} M dexamethasone, 37.5 μg/ml ascorbate-2-phosphate, 1% sodium pyruvate, and 10 ng/ml TGF-β1.

Compression testing

The roll-up constructs with hMSCs were cultured for 21 days under differentiating conditions, and were then cut into four sections using a scalpel, and the thickness and diameter of each sample was measured. The compressive modulus of each sample was determined in a Rheometrics Solids Analyzer II (Piscataway, NJ). Each sample was compressed for 10 s at a strain rate of 1% s^{-1}, and compression tests were performed on 6 samples per condition. Stress (σ) vs. strain (ε) data were recorded by a computer data acquisition system, transferred to Excel, and fitted to the equation $\sigma = E_c\varepsilon$ to yield the construct modulus of elasticity (E_c) of the roll-up constructs [6, 18].

Furthermore, the compressive modulus of elasticity (E_t) values of the formed tissue of the roll-up constructs were calculated using the equation: $E_cA_c = E_tA_t + E_sA_s$. Here, E_s is the scaffold modulus of elasticity, and A_c, A_t, and A_s are the cross-sectional areas of the construct (formed tissue + scaffold), formed tissue and scaffold respectively. E_s value was obtained from the ratio of tissue to construct tensile modulus of elasticity from our previous study [15]; we assumed that the compressive modulus of elasticity would display a similar ratio.

Histological and Immunohistochemical Analyses

After culturing for 21 days, samples were fixed in 4% neutral-buffered formaldehyde. Five micrometer thick sections were deparaffinized and used for the following. Toluidine blue and safranin O stainings were carried out as per previously published procedures [19]. To distinguish between sulfated and carboxylated GAGs, we also performed Alcian blue staining at a pH of 1 (sulfated GAG staining [20]) and at a pH of 2.5 (carboxylated GAG staining [21]). For type II collagen by immunohistochemistry, antigen unmasking was performed with 1 mg/mL pronase in PBS for 15 minutes at room temperature. After washing the samples with PBS twice for 30 minutes, they were then blocked with 10% normal goat serum (NGS) in PBS for 30 minutes. The primary antibodies were diluted 1: 50 in 1% NGS in PBS and were applied to the samples for 1 hour to stain for collagen type II. The samples were then washed with PBS (2 × 30 minutes). Fluorescein isothiocyanate (FITC)-conjugated goat anti-mouse IgG secondary antibody, diluted 1:500 in 1% NGS in PBS, was then applied to all samples for 45 minutes. The samples were again washed with PBS for 1 hour and wet-mounted using 5% N-propyl gallate in glycerol. Samples were imaged using either a SPOT RT or Leica digital camera attached to a Leica fluorescence microscope (Wetzlar, Germany).

Second Harmonic Generation (SHG) Imaging

Cell produced ECM inside the guidance channels of the 2-D constructs was observed by SHG microscopy using a Leica SP5 II MP-OPO microscope *(Leica Microsystems, GmbH,*

Author Manuscript Author Manuscript Author Manuscript Author Manuscript

Wetzlar, Germany). The excitation light source was a femtosecond pulsed Coherent Chameleon Vision II Ti:Sapphire multiphoton laser with optical parametric oscillation centered at 890 nm. The SHG signal was collected in the reverse direction using an internal hybrid photo detector (HyD™) with the spectral channel tuned to 425–465 nm and the confocal pinhole wide open. Images were collected using a water immersion objective (Leica: HCX IR APO L 40× 1.10 NA). Samples were imaged from the surface down to 45 micrometer deep (channel top area). Z-series of the channels were collected using a 1 μm step-size.

Collagen Fiber Alignment Analysis

To obtain a quantitative measure of collagen fiber alignment, the acute angle of collagen fibers of 10 micrometers and 20 micrometers lengths were measured relative to the direction of the length (longer dimension) of the channels. Raw images obtained using SHG imaging techniques were analyzed using Image-Pro Plus 6.2 software (Media Cybernetics, Rockville, MD) to determine collagen fiber alignment. A total of 51 collagen fibers within 100 micrometer channels with 100 micrometer spacing from 4 samples, 42 fibers within 100 micrometer channels with 50 micrometer spacing from 2 samples, and 69 collagen fibers from 3 control samples without channels were analyzed.

Polarized light microscopy

Polarized light microscopy was used to observe the collagen fiber alignment in 3-D roll-up constructs. For polarized light microscopy, the roll-up construct samples were fixed with 4% neutral-buffered formaldehyde overnight, and dehydrated in a graded ethanol series and embedded in paraffin. Sections of 15 micrometer thickness were stained with Sirius-Red as described previously [22]. Tissue in the channel of the 3-D constructs was imaged under polarized light microscopy.

Metabolism Analysis

We carried out glucose and lactate measurements to evaluate tissue metabolism and nutrient transport. Aliquots of culture medium (n=5 per condition) were sampled every other day during medium changes and were stored at −20°C. Glucose concentration in the medium was determined using an Accu-Chek Aviva meter (Roche Diagnostics, Indianapolis, IN), with a detection range: 10 to 600 mg/dL. Lactate concentration was obtained using a Lactate Scout meter (SensLab GmbH Leipzig, Germany), with a detection range: 0.5 to 25 mmol/l. 10 μl and 20 μl of medium were used to measure glucose and lactate concentrations respectively.

Statistical Methods

For all quantitative results, statistical analysis was carried out using the Origin 8.5.1 (Origin Lab, Northampton, MA) software package. Pairwise comparisons were performed by Tukey's test to compare data groups. For comparisons between distributions shown in Fig 5, we used the Mann-Whitney test. Unless specified, a p value of less than 0.05 was used to determine statistical significance. Where necessary, sample sizes are indicated in the figure legends.

Author Manuscript Author Manuscript Author Manuscript Author Manuscript

Results

Roll-up Method

The roll-up method was a simple and effective way to form large constructs from a thin layer of construct containing microscale guidance features and seeded with cells (Fig. 1). Cell seeding on top of a thin layer construct was easy and straightforward. Integration of multiple layers of scaffold occurred in all constructs during the roll-up process (Fig. 2). Due to the technique used in the roll-up method, the number of spiral turns ranged from 4 to 6 for all constructs. Both cross and longitudinal sections showed integration of scaffolds by the cells (Fig. 2). The roll-up constructs were easy to handle, and the smaller constructs cut from them had very good mechanical integrity as evidenced by their mechanical properties (see *Mechanical Properties*).

ECM Production

Intense toluidine blue staining, indicating robust GAG deposition, was demonstrated in the outer 3 tissue layers and parts of the fourth layer from the outside of the constructs (Fig. 2A–2C, 2a–2c). Cells were distributed throughout these outer 3–4 layers of the scaffold. Similar results were found in all constructs: controls, constructs with microscale guidance channels. A sparse number of cells and amount of ECM were distributed after the fourth layer from the outside. ECM deposition in constructs with microchannels (Fig. 2B, 2C, 2b, 2c) seemed to be more distributed in the outer 3 tissue layers compared to other layers. The light staining at the tissue interior as shown in Fig. 2b is due to the collagen scaffold that contained GAG. In contrast, constructs without the channels displayed non-uniform ECM distribution within all the different layers (Fig. 2A, 2a).

Immunohistochemistry of the roll-up constructs cultured for 21 days in chondrogenic medium showed strong positive staining for collagen type II (Fig. 3B, 3D) that matched with the GAG staining (Fig. 3A, 3C). Dense ECM rich in both GAG and type II collagen throughout the outer 3 layers of the constructs can be seen. ECM accumulated and filled the gap between the scaffold layers, displaying excellent tissue-scaffold integration (Yellow arrows, Fig. 3C). Figure 4 shows that GAG formed in microchannels containing tissue comprised of both sulfated (Fig. 4A) and carboxylated (Fig. 4B) GAGs. Safranin-O (Fig. 4C) and toluidine blue (Fig. 4D) staining shows total GAGs in the tissue. Similar results were obtained in tissue with no microchannels (data not shown).

Collagen Fiber Alignment

Second harmonic generation (SHG) imaging was used to visualize the collagen fibers within the guidance channels of hMSC constructs containing 100 micrometer guidance channels separated by 50 micrometers, cultured in chondrogenic medium for 21 days. Collagen fibers synthesized during hMSC differentiation within the microchannels displayed alignment along the length of the channels of the 3-D constructs (blue arrowheads Fig. 5B), while collagen fibers in constructs without channels did not display any preferential alignment (Fig. 5A). Results of alignment angle distribution (Fig. 5C) within both controls and microchannels containing constructs show that the microchannels led to improved alignment ($p<0.0001$) in the resultant 3-D constructs.

Author Manuscript Author Manuscript Author Manuscript Author Manuscript

The SHG imaging results are verified by Sirius-red staining of longitudinal sections tissue constructs containing 100 micrometer guidance channels separated by 50 micrometers (Fig. 5D). Thick collagen fibers (orange/yellowish) (blue arrowheads in Fig. 5D) and thin collagen fibers (green or yellow green) (Fig. 5D) were deposited in the constructs. Importantly, cell produced collagenous fibers were aligned along the length of the 100 micrometer guidance channels.

Metabolism Analysis

Glucose consumption rate and lactate production rate for constructs during 21 days in chondrogenic culture were measured (Fig. 6). The per cell glucose consumption rate (Fig. 6A) significantly decreased ($p < 0.05$) from day 3 to day 7 for constructs containing 100 micrometer channels with 50 micrometer spacing (174 ± 4 (mean ± standard error of the mean) fmole/hr to 104 ± 4 fmole/hr) (Fig. 6A: 100C_50S), constructs containing 100 micrometer channels with 100 micrometer spacing (171 ± 3 fmole/hr to 102 ± 9 fmole/hr) (Fig. 6A: 100C_100S), and control constructs without channels (172 ± 3 fmole/hr to 123 ± 3 fmole/hr) (Fig. 6A: Control). Similar results were obtained in lactate production rate measurements. The per-cell lactate production rate (Fig. 6B) significantly decreased ($p < 0.05$) from day 3 to day 7. The lactate production rate decreased from 259 ± 11 fmole/hr to 187 ± 5 fmole/hr for the 100C_50S constructs, from 257 ± 5 fmole/hr to 189 ± 6 fmole/hr for the 100C_100S constructs, and from 254.5 ± 5.9 fmole/hr to 194.9 ± 1.9 fmole/hr for the control constructs. There was no significant change in per cell glucose consumption rate and lactate production rate for all constructs from day 7 to day 21 ($p > 0.05$). In addition, there was no significant difference for the per cell glucose consumption rate between constructs with channels (100C_50S constructs, 100C_100S constructs) and constructs without channels (control) at day 3, day 7, day 15, and day 21 (Fig. 6A). Similar results were obtained in lactate production rate except for day 21, at which the lactate production rate in control constructs was slightly higher than that in constructs with channels (Fig. 6B)

Mechanical Properties

Without hMSCs, roll-up constructs formed from sheets with or without channels cultured over 21 days fell apart during testing (data not shown). As a result, we used hMSC constructs without guidance channels as controls. Roll-up constructs containing hMSCs within guidance channels (Fig. 7, Right Y-Axis: 100C_100S and 100C_50S) cultured for 21 days under differentiating conditions had significantly superior mechanical properties compared to corresponding constructs without channels (Fig. 7, Right Y-Axis: control) ($p < 0.05$). Tissue compressive modulus values were estimated (Eq. 1) and are shown (Fig. 7, Left Y-Axis) with similar results.

There was no significant difference in the mechanical properties between constructs containing 50 micrometer spacing (Fig. 7: 100C_50S) and constructs containing 100 micrometer spacing (Fig. 7: 100C_100S). However, the center of the constructs containing 100 micrometer spacing (Fig. 7: 100C_100S Center] had significantly higher compressive modulus values than the edge regions (Fig. 7: 100C_100S Edge), while constructs containing 50 micrometer spacing had no significant difference between the center and edge regions of the constructs (Fig. 7: 100C_50S). Constructs containing spacing of 50

Author Manuscript Author Manuscript Author Manuscript Author Manuscript

micrometer (Fig. 7: 100C_50S) resulted in more uniform compressive properties throughout the entire construct when compared to constructs with 100 micrometer spacing (Fig. 7: 100C_100S). This suggests that 100C_50S constructs have more evenly distributed tissue from the edge to the center of the construct than the 100C_100S constructs, which was also observed via histology.

Discussion

In the present study, we developed a new method that utilized the microscale contact guidance of MSCs, which we investigated in our previous study, to produce a 3-D cartilage construct with an oriented microstructure and enhanced mechanical properties [15]. Previous studies in large animal models have shown that defects less than a critical size of 3 mm diameter may lead to complete spontaneous repair of articular cartilage, while repair attempts for larger defects result in fibrocartilage repair tissue that ultimately fails [23–26]. Current clinical techniques, such as microfracture and autologous matrix-induced chondrogenesis techniques, can initially relieve the symptoms for larger cartilage defects; however, these methods will also ultimately result in mechanically inferior fibrocartilage repair tissue and their long term utility is uncertain [27–29]. The latter technique combines microfracture technique with exogenous scaffolds and has shown promise [30]. Tissue engineering serves as a promising alternative to repair large cartilage defects. However, the production of a large scale tissue engineered constructs remains a challenge.

The size of the constructs (1.8 cm (length) × 0.35 cm (diameter), Fig. 1) that were produced using the roll-up method described here is significantly larger in thickness (length) compared to native cartilage tissue. This has the potential to treat multiple lesions by simple radial-sectioning of the rolled tissue and allows flexibility to the clinician. ECM within the constructs containing microchannels (100C_50S, 100C_100S) were more uniformly distributed than the 3-D constructs without channels (Control) (Fig. 2). The hMSCs in constructs without the microchannels (Control) tended to aggregate into clumps in certain regions. We believe that the uneven distribution of ECM within the control roll-up constructs was caused by this tendency of the hMSCs to aggregate on scaffolds without channels. We hypothesize that the channels allow for more uniform cellular seeding and also help anchor the cells in place, therefore, preventing aggregation and rounding.

Our results show that ECM produced in the interior of the roll-up constructs is not homogenous. We believe that this is due to low glucose availability in the interior due to glucose mass transport limitations. Glucose metabolism has been reported to be an important factor in cartilage tissue engineering; glucose consumption and lactate production rates have been regarded as indicators for monitoring cell metabolism and matrix synthesis [31–35]. Our results (Fig. 6) show that the normalized glucose and lactose rates in the roll-up constructs are about 50% lower compared to those observed in hMSC aggregates [36, 37]. The difference in the rates may be due to the different systems (scaffold free pellet culture and collagen-GAG based constructs) since cellular biosynthetic activity is dependent on the biomaterial used. The difference, however, is likely due to transport limitations in the large construct. Low glucose availability could also affect cell viability though initial cell seeding was uniform across all constructs. The mass transport limitations can be addressed by

Author Manuscript Author Manuscript Author Manuscript Author Manuscript

reducing the length of the constructs from 2 cm to 3–4 mm (approximate thickness of knee cartilage). This would lead to transport of glucose in the axial direction additionally thus greatly enhancing transport. The ratio of lactate production to glucose consumption is ideally 2 for anaerobic glycolysis. Teixeira *et al.* reported a ratio of 2 for single chondrocytes cultured in hydrogels and 1 for aggregate culture [38]. The ratio for the roll-up constructs is approximately 1.6, which indicates that while anaerobic glycolysis dominates, a part of the glucose uptake was used directly for GAG synthesis.

Our qualitative results (Fig. 4) show that cells synthesized both carboxylated and sulfated GAGs. In adult hyaline cartilage, sulfated GAG content, on a weight basis, is more than an order of magnitude greater than the HA content. During development, however, it has been shown that non-sulfated disaccharide content starts higher than 4-sulfated GAG but decreases significantly with age [39]. Collectively, it suggests that the ECM formed is relatively ‘young’ compared to adult articular cartilage.

To further study collagen fibers at the tissue level for the constructs, polarized light microscopy and SHG images revealed cell produced collagenous matrix in the constructs and collagen fibers aligned along the channel length (Fig. 5). These results further confirm our hypothesis in 3-D constructs that microscale substrate features cause differentiating MSCs to preferentially arrange themselves and to deposit an oriented cartilage ECM. We have shown that MSCs align and elongate along the length of the small guidance channels in our previous study [15], and now demonstrate that collagenous matrix produced in 3-D roll-up constructs can also be aligned (Fig. 5). Cells are able to manipulate the ECM around them into a specific architecture via cell motility activity and cell produced contraction force [40, 41]. By utilizing microchannels in these 3-D constructs, we were able to create cartilage tissue with aligned ECM architecture that displayed alignment along the length of the channels (perpendicular to the cross section of the constructs). This alignment is similar to the deep zone of native articular cartilage, in which the collagen fibers are aligned perpendicular to the subchondral bone. This collagen fiber arrangement has been shown to improve the compressive properties of native cartilage and having both perpendicular (deep zone) and parallel (superficial zone) arrangements of microchannels in the scaffold can help achieve a construct with improved properties [13, 14].

The tissue compressive elasticity modulus for the constructs containing guidance channels ranged from 1.2 to 2.1 MPa (Fig. 7), which is in the lower range of native articular cartilage properties found in the literature (1.2 to 7.8 MPa) [42, 43]. Roll-up constructs containing microscale guidance channels displayed superior mechanical properties when compared to constructs without guidance channels. Since cell seeding efficiencies are high and similar across all the constructs, this suggests that microscale guidance has an effect on the mechanical function of the resulting tissue within 3-D constructs. The compressive elasticity modulus for the ‘center’ region of the roll-up construct (Fig. 7) was generally higher than the compressive elasticity modulus for the edge region, which may be a result of the hypoxic environment within the center of the constructs [44–47]. Kanichai *et al.* reported that MSC culture under hypoxia displayed a significant increase in proteoglycan deposition and collagen type II expression after 3 weeks in culture [46]. We hypothesize that the hypoxic conditions within the center region of the constructs led to enhanced mechanical properties.

Author Manuscript Author Manuscript Author Manuscript Author Manuscript

Current 3-D tissue engineered cartilage, fabricated using stem cells and various types of scaffolds including poly(e-caprolactone), poly(L-lactic acid), collagen type I, hyaluronic acid hydrogels, gelatin, alginate, and agarose, typically displays a compressive elasticity modulus between 10–15 kPa [48–50]. Our constructs containing guidance channels displayed a compressive modulus elasticity modulus values superior to most current tissue engineered cartilage constructs. Improving mechanical properties is critical for clinical translatability as they should lead to better mechanical integration with the native tissue. Large mechanical mismatches between construct and native tissue will likely lead to inferior performance clinically [51].

Our study demonstrated that we can form large scale constructs from thin membranes of cell-containing microchannels leading to significantly improved mechanical properties. However, our study has certain limitations. First, while native cartilage possesses a compressive elasticity modulus that varies from 1.2 to 7.8 MPa, the roll-up constructs only reached the initial range of native cartilage [42]. This limitation of our constructs may be due to the hole along the center of the construct and local areas of poor integration between the scaffold and tissue. In future studies, we will investigate methods to eliminate the central cylindrical hole and to enhance integration between the scaffold and tissue. However, despite this limitation, we have created a large scale 3-D cartilage construct that displays enhanced mechanical properties compared to most current tissue engineered constructs and that shows promise for future clinical applications.

Conclusions

In this work, we successfully created structurally oriented 3-D cartilage-like tissue for *in vivo* applications by rolling up 2-D hMSC-seeded collagen-GAG based scaffolds to form 3-D roll-up tissue with microscale architecture to guide the differentiating hMSCs to deposit structurally oriented ECM. Roll-up constructs containing microchannels displayed superior mechanical and tissue properties among all constructs. Dense ECM rich in both GAG and type II collagen throughout the outer 3 layers of the construct was observed in these constructs. Importantly, we demonstrated that microscale guidance channels incorporated within the 3-D cartilage constructs led to the production of aligned cell-produced collagenous matrix and enhanced mechanical function. These constructs display enhanced mechanical properties compared to current tissue engineered cartilage and will be further investigated for future *in vivo* testing.

Acknowledgments

We thank Dr. Don Lennon, Amad Awadallah, and Lori Duesler of the Skeletal Research Center, Department of Biology, Case Western Reserve University, Cleveland, OH for help with the MSC isolation and culture, sectioning and histology, and immunohistochemistry respectively. The above work was funded by grants from the National Institutes of Health (AR053622 and EB021911). Dr. Alexander L. Rivera was supported in part by the National Science Foundation Graduate Research Fellowship under Grant No. 0951783

References

1. Chung C, Burdick JA. Influence of three-dimensional hyaluronic acid microenvironments on mesenchymal stem cell chondrogenesis. Tissue Engineering Part A. 2009; 15:243–54. [PubMed: 19193129]

Author Manuscript Author Manuscript Author Manuscript Author Manuscript

2. Dickhut A, Gottwald E, Steck E, Heisel C, Richter W. Chondrogenesis of mesenchymal stem cells in gel-like biomaterials in vitro and in vivo. Frontiers in Bioscience. 2008; 13:4517–28. [PubMed: 18508526]

3. Djouad F, Mrugala D, Noel D, Jorgensen C. Engineered mesenchymal stem cells for cartilage repair. Regenerative Medicine. 2006; 1:529–37. [PubMed: 17465847]

4. Jakobsen RB, Shandadfar A, Reinholt FP, Brinchmann JE. Chondrogenesis in a hyaluronic acid scaffold: Comparison between chondrocytes and msc from bone marrow and adipose tissue. Knee Surgery Sports Traumatology Arthroscopy. 2010; 18:1407–16.

5. Janjanin S, Li WJ, Morgan MT, Shanti RA, Tuan RS. Mold-shaped, nanofiber scaffold-based cartilage engineering using human mesenchymal stem cells and bioreactor. Journal of Surgical Research. 2008; 149:47–56. [PubMed: 18316094]

6. Liang WH, Kienitz BL, Penick KJ, Welter JF, Zawodzinski TA, Baskaran H. Concentrated collagen-chondroitin sulfate scaffolds for tissue engineering applications. Journal of Biomedical Materials Research Part A. 2010; 94A:1050–60.

7. Spadaccio C, Rainer A, Trombetta M, Vadala G, Chello M, Covino E, Denaro V, Toyoda Y, Genovese JA. Poly-l-lactic acid/hydroxyapatite electrospun nanocomposites induce chondrogenic differentiation of human msc. Annals of Biomedical Engineering. 2009; 37:1376–89. [PubMed: 19418224]

8. Wang YZ, Kim UJ, Blasioli DJ, Kim HJ, Kaplan DL. In vitro cartilage tissue engineering with 3d porous aqueous-derived silk scaffolds and mesenchymal stem cells. Biomaterials. 2005; 26:7082–94. [PubMed: 15985292]

9. Wang YZ, Blasioli DJ, Kim HJ, Kim HS, Kaplan DL. Cartilage tissue engineering with silk scaffolds and human articular chondrocytes. Biomaterials. 2006; 27:4434–42. [PubMed: 16677707]

10. Xue JX, Gong YY, Zhou GD, Liu W, Cao Y, Zhang WJ. Chondrogenic differentiation of bone marrow-derived mesenchymal stem cells induced by acellular cartilage sheets. Biomaterials. 2012; 33:5832–40. [PubMed: 22608213]

11. Yang Q, Peng J, Guo Q, Huang J, Zhang L, Yao J, Yang F, Wang S, Xu W, Wang A, Lu S. A cartilage ecm-derived 3-d porous acellular matrix scaffold for in vivo cartilage tissue engineering with pkh26-labeled chondrogenic bone marrow-derived mesenchymal stem cells. Biomaterials. 2008; 29:2378–87. [PubMed: 18313139]

12. Zwingmann J, Mehlhorn AT, Suedkamp N, Stark B, Dauner M, Schmal H. Chondrogenic differentiation of human articular chondrocytes differs in biodegradable pga/pla scaffolds. Tissue Engineering. 2007; 13:2335–43. [PubMed: 17691868]

13. Wilson W, Huyghe JM, van Donkelaar CC. Depth-dependent compressive equilibrium properties of articular cartilage explained by its composition. Biomechanics and Modeling in Mechanobiology. 2007; 6:43–53. [PubMed: 16710737]

14. Shirazi R, Shirazi-Adl A, Hurtig M. Role of cartilage collagen fibrils networks in knee joint biomechanics under compression. Journal of Biomechanics. 2008; 41:3340–8. [PubMed: 19022449]

15. Chou CL, Rivera AL, Sakai T, Caplan AI, Goldberg VM, Welter JF, Baskaran H. Micrometer scale guidance of mesenchymal stem cells to form structurally oriented cartilage extracellular matrix. Tissue engineering Part A. 2013; 19:1081–90. [PubMed: 23157410]

16. Janakiraman V, Kienitz BL, Baskaran H. Lithography technique for topographical micropatterning of collagen-glycosaminoglycan membranes for tissue engineering applications. J Med Device. 2007; 1:233–7. [PubMed: 19823602]

17. Welter JF, Solchaga LA, Penick KJ. Simplification of aggregate culture of human mesenchymal stem cells as a chondrogenic screening assay. Biotechniques. 2007; 42:732, 4–7. [PubMed: 17612296]

18. Woo SLY, Akeson WH, Jemmott GF. Measurements of nonhomogeneous, directional mechanical properties of articular cartilage in tension. Journal of Biomechanics. 1976; 9:785–91. [PubMed: 1022791]

19. Pastoureau P, Chomel A. Methods for cartilage and subchondral bone histomorphometry. Methods Mol Med. 2004; 101:79–91. [PubMed: 15299211]

Author Manuscript Author Manuscript Author Manuscript Author Manuscript

20. Ravetto C. Alcian blue-alcian yellow: A new method for the identification of different acidic groups. Journal of Histochemistry & Cytochemistry. 1964; 12:44. [PubMed: 14187307]
21. Green MR, Pastewka JV. Simultaneous differential staining by a cationic carbocyanine dye of nucleic acids, proteins and conjugated proteins. Ii. Carbohydrate and sulfated carbohydrate-containing proteins. J Histochem Cytochem. 1974; 22:774–81. [PubMed: 4137192]
22. Moriya K, Bae E, Honda K, Sakai K, Sakaguchi T, Tsujimoto I, Kamisoyama H, Keene DR, Sasaki T, Sakai T. A fibronectin-independent mechanism of collagen fibrillogenesis in adult liver remodeling. Gastroenterology. 2011; 140:1653–63. [PubMed: 21320502]
23. Convery FR, Akeson WH, Keown GH. The repair of large osteochondral defects. An experimental study in horses. Clinical orthopaedics and related research. 1972; 82:253–62. [PubMed: 5011034]
24. Jackson DW, Lalor PA, Aberman HM, Simon TM. Spontaneous repair of fullthickness defects of articular cartilage in a goat model - a preliminary study. Journal of Bone and Joint Surgery-American. 2001; 83A:53–64.
25. Shapiro F, Koide S, Glimcher MJ. Cell origin and differentiation in the repair of fullthickness defects of articular-cartilage. Journal of Bone and Joint Surgery-American. 1993; 75A:532–53.
26. ButnariuEphrat M, Robinson D, Mendes DG, Halperin N, Nevo Z. Resurfacing of goat articular cartilage by chondrocytes derived from bone marrow. Clinical orthopaedics and related research. 1996:234–43.
27. Blevins FT, Steadman JR, Rodrigo JJ, Silliman J. Treatment of articular cartilage defects in athletes: An analysis of functional outcome and lesion appearance. Orthopedics. 1998; 21:761–7. discussion 7–8. [PubMed: 9672913]
28. Benthien JP, Behrens P. Autologous matrix-induced chondrogenesis (amic). A one-step procedure for retropatellar articular resurfacing. Acta Orthop Belg. 2010; 76:260–3. [PubMed: 20503954]
29. Benthien JP, Behrens P. Autologous matrix-induced chondrogenesis (amic): Combining microfracturing and a collagen i/iii matrix for articular cartilage resurfacing. Cartilage. 2010; 1:65–8. [PubMed: 26069536]
30. Lee YH, Suzer F, Thermann H. Autologous matrix-induced chondrogenesis in the knee: A review. Cartilage. 2014; 5:145–53. [PubMed: 26069694]
31. Lee RB, Wilkins RJ, Razaq S, Urban JPG. The effect of mechanical stress on cartilage energy metabolism. Biorheology. 2002; 39:133–43. [PubMed: 12082276]
32. Lee RB, Urban JPG. Evidence for a negative pasteur effect in articular cartilage. Biochemical Journal. 1997; 321:95–102. [PubMed: 9003406]
33. Lane JM, Brighton CT, Menkowitz BJ. Anaerobic and aerobic metabolism in articular-cartilage. Journal of Rheumatology. 1977; 4:334–42. [PubMed: 604473]
34. Otte P. Basic cell-metabolism of articular-cartilage - manometric studies. Zeitschrift Fur Rheumatologie. 1991; 50:304–12. [PubMed: 1776367]
35. Nettles DL, Chilkoti A, Setton LA. Early metabolite levels predict long-term matrix accumulation for chondrocytes in elastin-like polypeptide biopolymer scaffolds. Tissue Engineering Part A. 2009; 15:2113–21. [PubMed: 19193139]
36. Pattappa G, Heywood HK, De Bruijn JD, Lee DA. The metabolism of human mesenchymal stem cells during proliferation and differentiation. J Cell Physiol. 226:2562–70.
37. Pattappa G, Heywood HK, De Bruijn JD, Lee DA. The metabolism of human mesenchymal stem cells during proliferation and differentiation. Journal of Cellular Physiology. 2011; 226:2562–70. [PubMed: 21792913]
38. Teixeira LSM, Leijten JCH, Sobral J, Jin R, van Apeldoorn AA, Feijen J, van Blitterswijk C, Dijkstra PJ, Karperien M. High throughput generated micro-aggregates of chondrocytes stimulate cartilage formation in vitro and in vivo. European Cells & Materials. 2012; 23:387–99. [PubMed: 22665161]
39. Roughley PJ, White RJ, Glant TT. The structure and abundance of cartilage proteoglycans during early development of the human fetus. Pediatr Res. 1987; 22:409–13. [PubMed: 3120142]
40. Lee GM, Loeser RF. Cell surface receptors transmit sufficient force to bend collagen fibrils. Experimental Cell Research. 1999; 248:294–305. [PubMed: 10094835]
41. Ohsawa S, Yasui N, Ono K. Contraction of collagen gel by the dedifferentiated chondrocytes. Cell Biology International Reports. 1982; 6:767–74. [PubMed: 7127487]

Author Manuscript Author Manuscript Author Manuscript Author Manuscript

42. Chen SS, Falcovitz YH, Schneiderman R, Maroudas A, Sah RL. Depth-dependent compressive properties of normal aged human femoral head articular cartilage: Relationship to fixed charge density. Osteoarthritis and Cartilage. 2001; 9:561–9. [PubMed: 11520170]

43. Setton LA, Elliott DM, Mow VC. Altered mechanics of cartilage with osteoarthritis: Human osteoarthritis and an experimental model of joint degeneration. Osteoarthritis and Cartilage. 1999; 7:2–14. [PubMed: 10367011]

44. Pfander D, Gelse K. Hypoxia and osteoarthritis: How chondrocytes survive hypoxic environments. Current Opinion in Rheumatology. 2007; 19:457–62. [PubMed: 17762611]

45. Lennon DP, Edmison JM, Caplan AI. Cultivation of rat marrow-derived mesenchymal stem cells in reduced oxygen tension: Effects on in vitro and in vivo osteochondrogenesis. Journal of Cellular Physiology. 2001; 187:345–55. [PubMed: 11319758]

46. Kanichai M, Ferguson D, Prendergast PJ, Campbell VA. Hypoxia promotes chondrogenesis in rat mesenchymal stem cells: A role for akt and hypoxia-inducible factor (hif)-1 alpha. Journal of Cellular Physiology. 2008; 216:708–15. [PubMed: 18366089]

47. Grayson WL, Zhao F, Izadpanah R, Bunnell B, Ma T. Effects of hypoxia on human mesenchymal stem cell expansion and plasticity in 3d constructs. Journal of Cellular Physiology. 2006; 207:331–9. [PubMed: 16331674]

48. Huang AH, Farrell MJ, Mauck RL. Mechanics and mechanobiology of mesenchymal stem cell-based engineered cartilage. Journal of Biomechanics. 2011; 43:128–36.

49. Awad HA, Wickham MQ, Leddy HA, Gimble JM, Guilak F. Chondrogenic differentiation of adipose-derived adult stem cells in agarose, alginate, and gelatin scaffolds. Biomaterials. 2004; 25:3211–22. [PubMed: 14980416]

50. Bian L, Zhai DY, Tous E, Rai R, Mauck RL, Burdick JA. Enhanced msc chondrogenesis following delivery of tgf-beta 3 from alginate microspheres within hyaluronic acid hydrogels in vitro and in vivo. Biomaterials. 2011; 32:6425–34. [PubMed: 21652067]

51. Kelly DJ, Prendergast PJ. Prediction of the optimal mechanical properties for a scaffold used in osteochondral defect repair. Tissue Eng. 2006; 12:2509–19. [PubMed: 16995784]

Author Manuscript Author Manuscript Author Manuscript Author Manuscript

Statement of Significance

Tissue engineered cartilage constructs made with human mesenchymal stem cells (hMSCs), scaffolds and bioactive factors are a promising solution to treat cartilage defects. A major disadvantage of these constructs is their inferior mechanical properties compared to the native tissue, which is likely due to the lack of structural organization of the extracellular matrix of the engineered constructs. In this study, we developed three-dimensional (3-D) cartilage constructs from rectangular scaffold sheets containing hMSCs in micro-guidance channels and characterized their mechanical properties and metabolic requirements. The work led to a novel roll-up method to embed 2-D microscale structures in 3-D constructs. Further, micro-guidance channels incorporated within the 3-D cartilage constructs led to the production of aligned cell-produced matrix and enhanced mechanical function.

Author Manuscript Author Manuscript Author Manuscript Author Manuscript

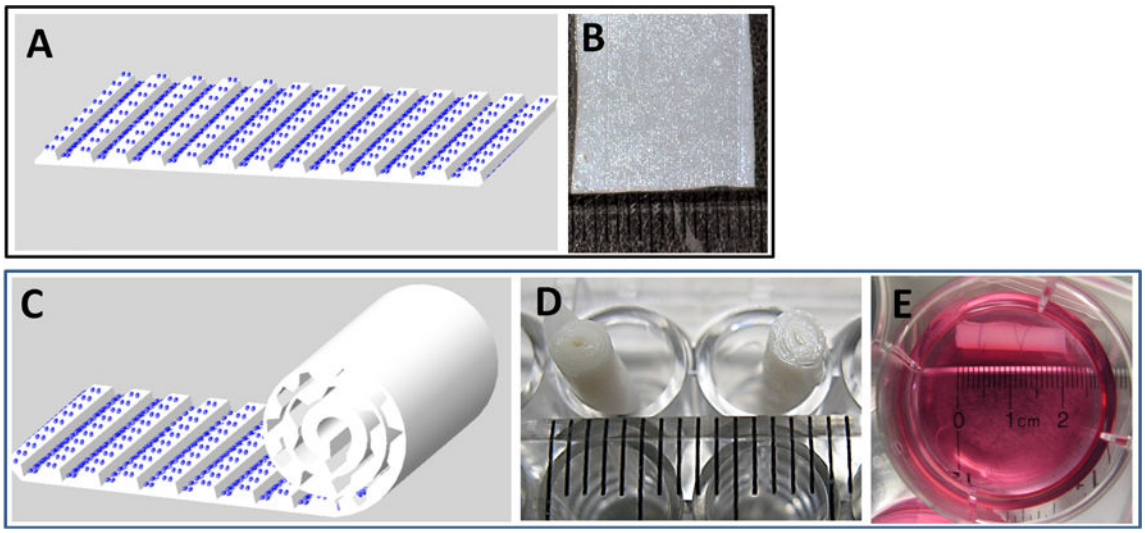

Figure 1.

Illustration of the roll-up process. (A, B) MSCs are seeded on to a collagen-GAG membrane containing microchannels. (C) Rolling direction is perpendicular to longitudinal direction of the channels. (D, E) Digital images of the cultured constructs.

Author Manuscript Author Manuscript Author Manuscript Author Manuscript

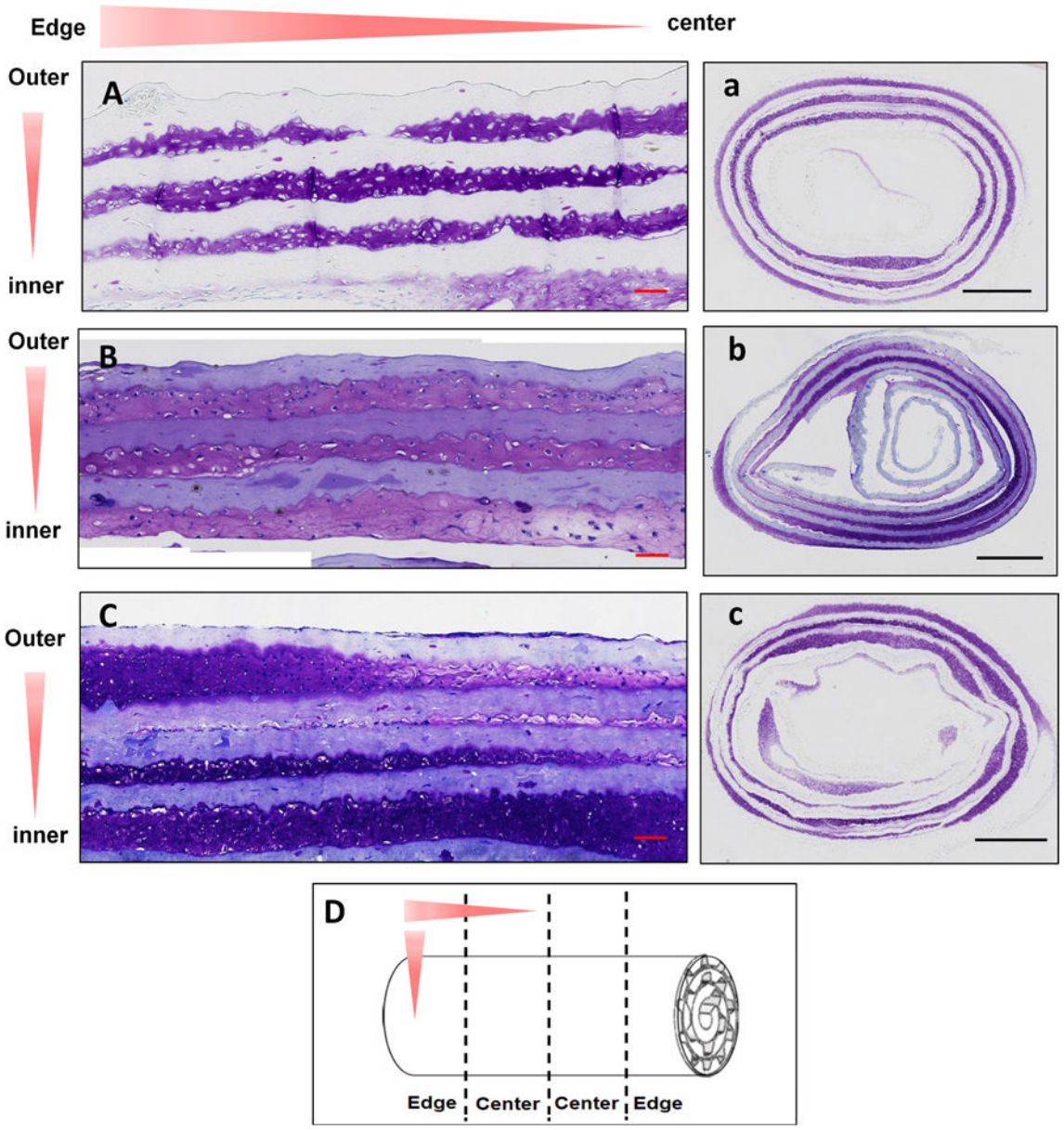

Figure 2.

Histology results. Sample constructs were sectioned in longitudinal and cross-sectional (D) and stained with toluidine blue for GAG staining. Sectional and sample orientations are shown using red arrows. A, B and C are longitudinal and a, b, c are cross-sectional images of samples with no channels (A, a), 100 micrometer channels with 100 micrometers between them (B, b) and 100 micrometer channels with 50 micrometers between them (C, c). Scale bars: 100 micrometers (A, B, C) and 1 mm (a, b, c)

Author Manuscript Author Manuscript Author Manuscript Author Manuscript

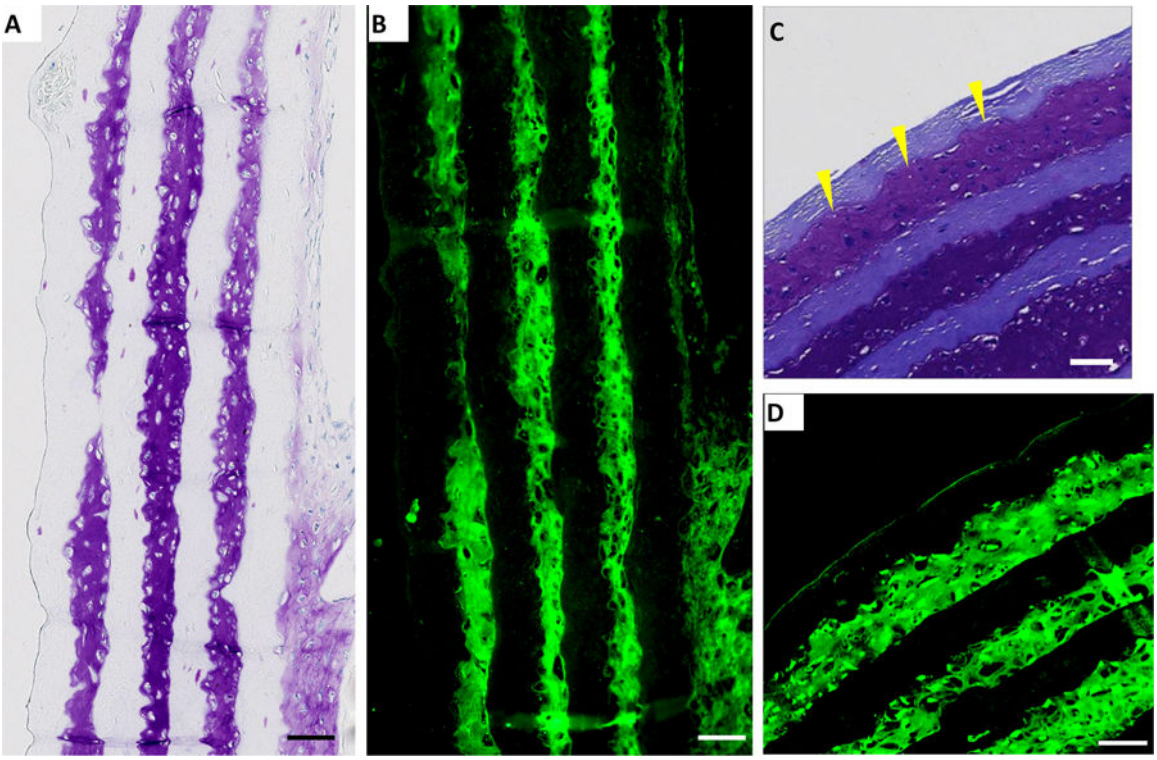

Figure 3.

Immunohistochemistry results. Sample constructs were sectioned in (A, B) longitudinal and (C, D) cross-sectional and stained for collagen type II (green, B, D) using immunochemical methods. Toluidine blue stained sections (A, C) are shown for comparison. A and B are sections from control constructs with no microchannels, C and D are sections from constructs containing 100 micrometer-wide channels with 100 micrometers spacing. Scale bar: 100 micrometers.

Author Manuscript Author Manuscript Author Manuscript Author Manuscript

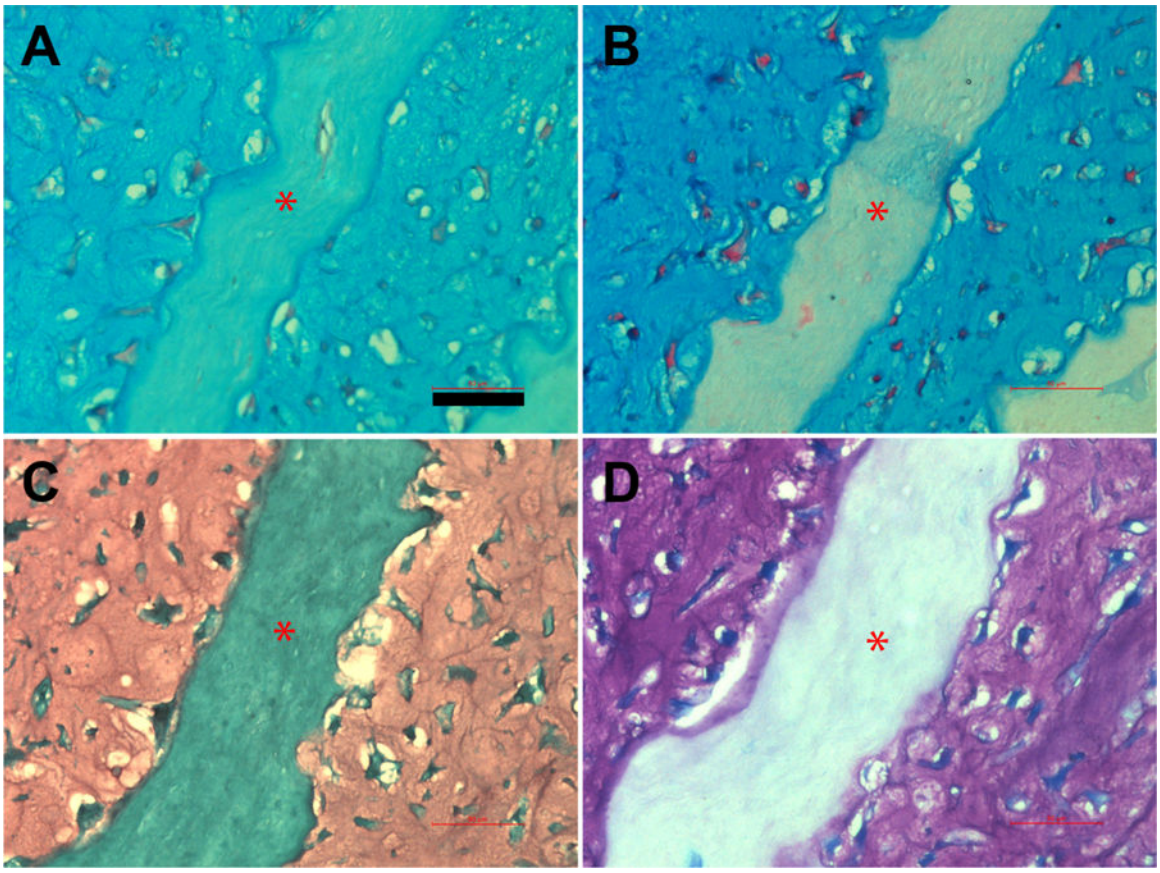

Figure 4.

Histology results for GAG distinction. Sample constructs were sectioned in longitudinal direction and stained with Alcian blue at pH 1 (A) and pH 2.5 (B), safranin O (C) and toluidine blue (D). The sections are from constructs containing 100 micrometer-wide channels with 100 micrometers spacing. Red stars indicate scaffold layer. Scale bar: 50 micrometers

Author Manuscript Author Manuscript Author Manuscript Author Manuscript

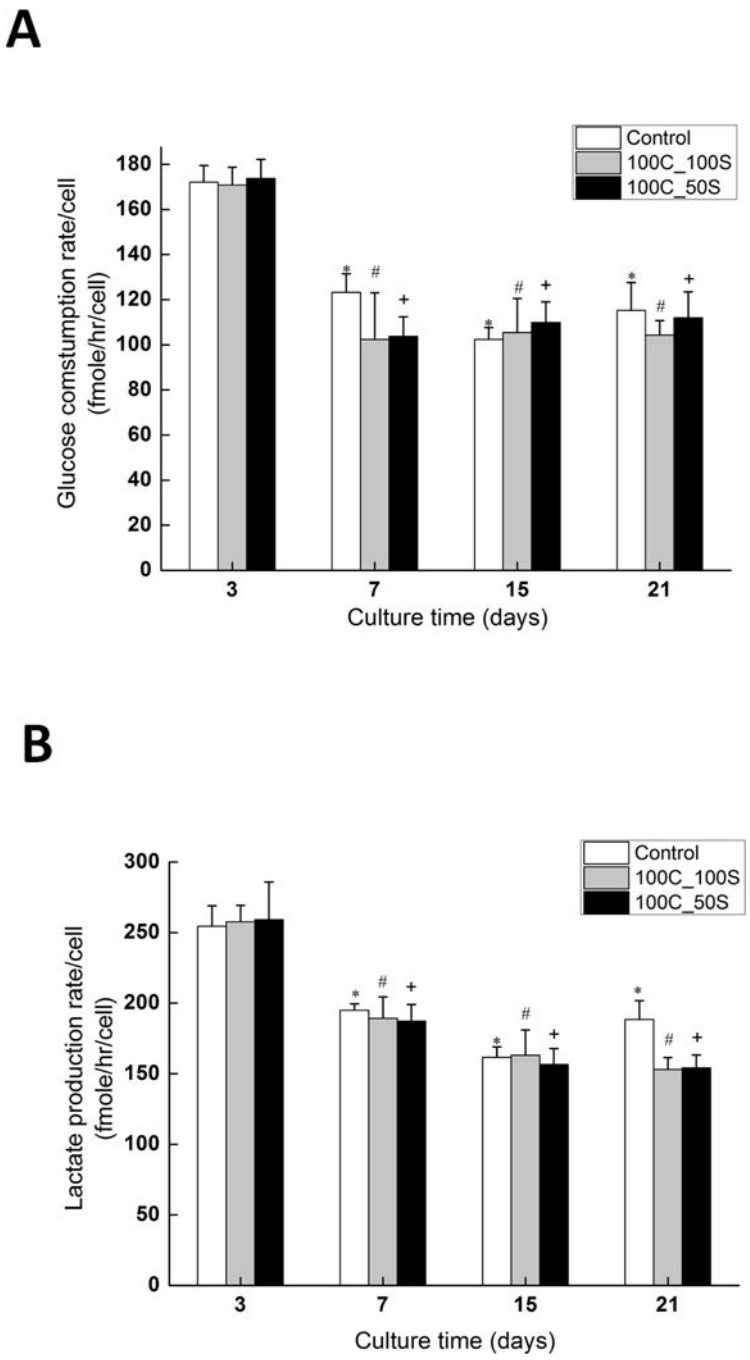

Figure 5.

Collagen fiber alignment. Second-harmonic images of (A) cartilage construct sections with no microchannels and (B) cartilage construct sections containing 100 micrometer channels with 100 micrometer spacing between them. (C) Frequency histogram of the angles of alignment in later constructs. An angle of 0° indicates perfect collagen fiber alignment along the length of the channel. Distributions of fiber angles in microchannels were significantly different compared to that of controls (Mann-Whitney test, $p<0.00001$) (D) Sirius red staining of the construct sections containing 100 micrometer channels with 100 micrometer

spacing between them. Red and black stars indicate scaffolds and blue arrows indicate aligned type II collagen fibers. Scale bars: 100 micrometers.

Author Manuscript Author Manuscript Author Manuscript Author Manuscript

Author Manuscript Author Manuscript Author Manuscript Author Manuscript

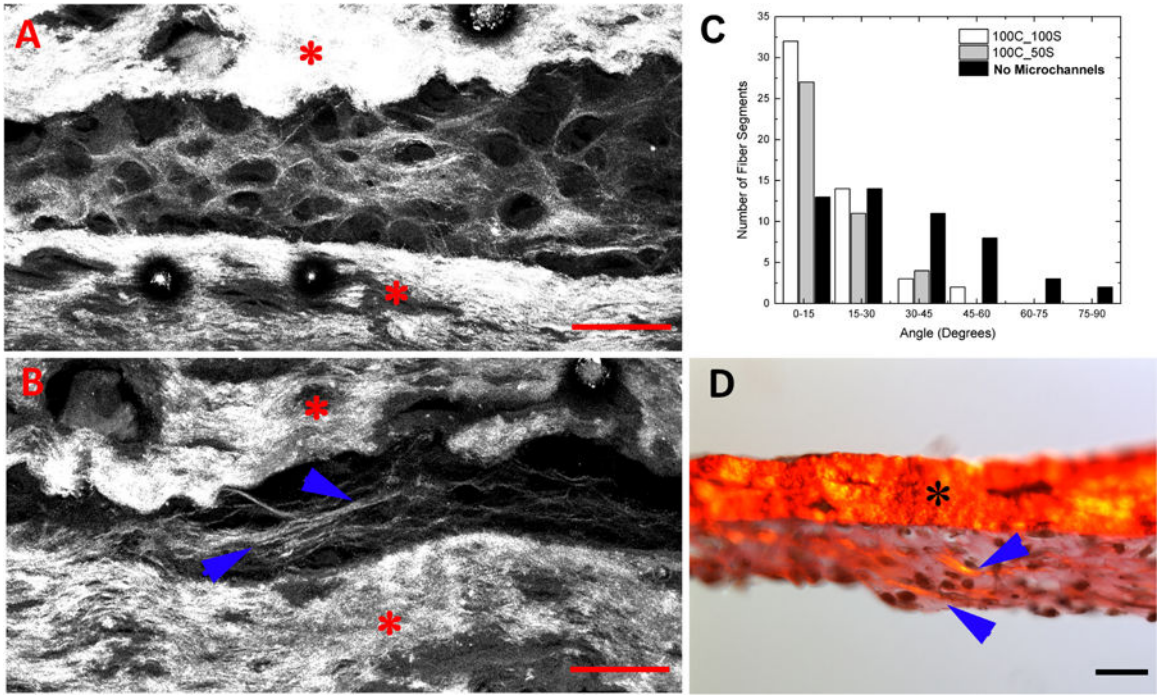

Figure 6.

Metabolism results. (A) Glucose consumption rate and (B) lactate production rate of constructs at different time points. 'Control' constructs had no microchannels, '100C_100S' represents constructs containing 100 micrometer channels with 100 micrometers spacing between them. '100C_50S' represents constructs containing 100 micrometer channels with 50 micrometers spacing between them. Five samples were used for each condition. Error bars represent the standard error of mean. *, # and + denote statistically significant difference from corresponding values from Day 3 ($p<0.05$).

Author Manuscript Author Manuscript Author Manuscript Author Manuscript

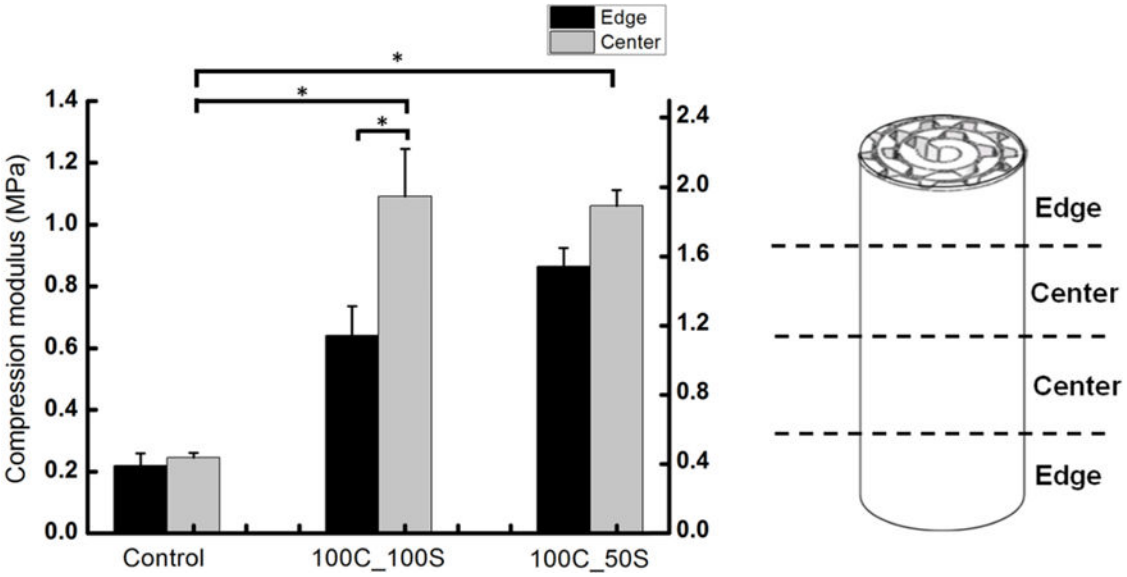

Figure 7.

Mechanical properties. Experimental values of compressive modulus of elasticity of constructs, E_c, (Left Y-Axis) and estimated values of compressive modulus of elasticity of formed tissue, E_t, (Right Y-Axis) are shown at two different locations ('Edge' and 'Center') 'Control' constructs had no microchannels, '100C_100S' represents constructs containing 100 micrometer channels with 100 micrometers spacing between them. '100C_50S' represents constructs containing 100 micrometer channels with 50 micrometers spacing between them. At least eight samples were used per condition and the error bars indicate the standard error of the mean.* denotes statistically significant difference ($p<0.05$).